

Anapole Moment of Majorana Fermions and Implications for Direct Detection of Neutralino Dark Matter

Alejandro Ibarra^a Merlin Reichard^a Ryo Nagai^b

^a*Physik-Department, Technische Universität München,
James-Frank-Straße, 85748 Garching, Germany*

^b*Department of Physics, Osaka University, Toyonaka, Osaka 560-0043, Japan*

E-mail: ibarra@tum.de, m.reichard@tum.de,
nagai@het.phys.sci.osaka-u.ac.jp

ABSTRACT: For Majorana fermions the anapole moment is the only allowed electromagnetic multipole moment. In this work we calculate the anapole moment induced at one-loop by the Yukawa and gauge interactions of a Majorana fermion, using the pinch technique to ensure the finiteness and gauge-invariance of the result. As archetypical example of a Majorana fermion, we calculate the anapole moment for the lightest neutralino in the Minimal Supersymmetric Standard Model, and specifically in the bino, wino and higgsino limits. Finally, we briefly discuss the implications of the anapole moment for the direct detection of dark matter in the form of Majorana fermions.

Contents

1	Introduction	1
2	One-Loop Calculation of the Anapole Moment of a Majorana Fermion	2
3	Anapole Moment of the Lightest Neutralino in the MSSM	5
4	MSSM Scenarios	8
4.1	Pure lightest neutralino & heavy sfermions	8
4.2	Light sfermion scenarios	9
4.3	Mixed lightest neutralino & decoupled sfermions	11
4.4	General MSSM scenarios	13
5	Direct Dark Matter Detection Through the Anapole Moment	15
6	Conclusions	17
A	Particle Spectrum of the MSSM	18

1 Introduction

There is mounting evidence for the existence of dark matter in galaxies, clusters of galaxies and the Universe at large scale, possibly in the form of a population of new elementary particles, not contained in the Standard Model of Particle Physics (for reviews, see *e.g.* [1–4]). Astronomical and cosmological observations demonstrate that dark matter particles interact with the electromagnetic radiation much more weakly than the hadrons or the charged leptons, however observations do not require the dark matter particle to be completely decoupled from the photon.

As is well known, for an electrically neutral fermion, the Lorentz- and gauge symmetries allow a magnetic- and electric dipole moment, and an anapole moment [5–11]. For an electrically neutral complex vector, also electric and magnetic quadrupole moments exist in general [12–14]. Therefore, even if the dark matter particle is electrically neutral, it may couple to the photon via the different electromagnetic multipoles. In fact, if the dark matter particle has interactions with the Standard Model particles, as many models suggest, such electromagnetic multipoles will be generically generated at the quantum level. This interaction could play an important role in the direct detection of dark matter particles through the scattering with nuclei, as discussed in several works, *e.g.* [15–35].

In this paper we will concentrate on Majorana fermions as dark matter candidates. In this case, the invariance of the Majorana field under the charge conjugation operation only allows the anapole moment. Concretely, we will consider the lightest neutralino in

the Minimal Supersymmetric Standard Model (MSSM) as an archetype of Majorana dark matter. The gauge and Yukawa interactions of the lightest neutralino with the charged particles of the Standard Model will generate an anapole moment at the one loop level. In the pure bino limit, the dark matter particle is a singlet Majorana fermion that couples to the Standard Model fermions via a t-channel mediator (the sfermions). The anapole moment of the singlet Majorana fermion has been calculated in [23]. In the pure wino and higgsino limits (as well as in the mixed cases), the dark matter particle has $SU(2)_L$ charge and also interacts with the W -boson, and special care has to be taken in order to ensure the gauge invariance of the result.

Similar challenges have been found in the past in the calculation of the neutrino charge radius [36–40], or in the calculation of the off-shell magnetic form factors of quarks and leptons in non-Abelian gauge theories [38, 41–43], which naively yield gauge-dependent results. The gauge dependence, clearly unphysical, arises due to redundancies in the individual Green functions which are introduced by the gauge-fixing procedure. This problem was solved by introducing the so-called pinch technique [44–48], which consists in an algorithmic diagrammatic construction of physical subamplitudes by resumming topologically similar terms within an amplitude and ultimately defining a proper and physical vertex by including only vertex-like contributions (see [49] for a review). Furthermore, the resulting effective Green functions coincides with the one calculated using the background field method in the quantum Feynman gauge [50–52].

In this paper we will apply the background field method to calculate the anapole moment of a spin 1/2 Majorana fermion that interacts both via Yukawa couplings and via gauge couplings, showing explicitly that the result is finite and gauge invariant. The general result is presented in section 2. In section 3 we particularize our results to the lightest neutralino in the MSSM, and in section 4 we study some well motivated MSSM scenarios. Then, in section 5 we briefly discuss the prospects of detection of a Majorana dark matter candidate via its anapole moment in direct search experiments, and finally in section 6 we present our conclusions. We also include Appendix A summarizing the calculation of the particle mass eigenstates in terms of the interaction eigenstates in the MSSM.

2 One-Loop Calculation of the Anapole Moment of a Majorana Fermion

We consider a Majorana fermion, that we denote by χ , with mass m_χ . The interaction vertex of a Majorana fermion with the photon is restricted by the Lorentz- and gauge symmetries to be of the form [9–11]

$$M_\mu(q) = f_A(q^2)(q^2\gamma_\mu - q_\mu\not{q})\gamma_5, \quad (2.1)$$

where q_μ denotes the photon outgoing momentum and $f_A(q^2)$ is the anapole form factor. This interaction vertex generates at low momentum the C- and P-violating effective Lagrangian

$$\mathcal{L}_{\text{eff}} = \frac{\mathcal{A}}{2} \bar{\chi}\gamma_\mu\gamma_5\chi\partial_\nu F^{\mu\nu}, \quad (2.2)$$

where \mathcal{A} is the anapole moment, defined as the zero momentum limit of the anapole form factor:

$$\mathcal{A} = \lim_{q^2 \rightarrow 0} f_A(q^2). \quad (2.3)$$

Being χ electrically neutral, the interaction with the photon can only arise at the quantum level through a coupling with charged particles. In this work, we will consider the cases where χ interacts with a charged gauge boson and/or with a charged scalar.

We first consider a scenario where χ couples to a charged Dirac fermion, χ^\mp with mass m_{χ^\pm} , and an electrically charged gauge boson, V^\pm with mass m_V acquired through the spontaneous breaking of a gauge symmetry. The interaction Lagrangian reads:

$$\mathcal{L}_{\text{FFV}} = \bar{\chi} \gamma^\mu [v_L P_L + v_R P_R] \chi^- V_\mu^+ + \bar{\chi} [c_L^G P_L + c_R^G P_R] \chi^- G^+ + \text{h.c.}, \quad (2.4)$$

where G^\pm are the Goldstone bosons arising from the spontaneous symmetry breaking.

To calculate the anapole moment we employ the background field method (BFM) [50, 53]. Namely, we replace the photon with the background photon $\gamma \rightarrow \hat{\gamma}$ and the γVV -vertex with its BFM version in the quantum Feynman gauge. Explicitly, the triple gauge vertex reads [53]

$$i\hat{\Gamma}_{\gamma VV}^{\mu\nu\rho}(k_1, k_2, k_3) = -ie [g_{\nu\rho}(k_3 - k_2)_\mu + g_{\mu\nu}(k_2 - k_1 + k_3)_\rho + g_{\rho\mu}(k_1 - k_3 - k_2)_\nu], \quad (2.5)$$

while the gauge-gauge-Goldstone vertex reads:

$$i\hat{\Gamma}_{\gamma VG}^{\mu\nu}(k_1, k_2, k_3) = 0. \quad (2.6)$$

The one-loop diagrams relevant for the calculation of the anapole moment in the BFM are shown in fig. 1. We obtain¹:

$$\mathcal{A}_V = \frac{e}{96\pi^2 m_\chi^2} \left\{ 2 [|v_L|^2 - |v_R|^2] \mathcal{F}_V\left(\frac{m_{\chi^-}}{m_\chi}, \frac{m_V}{m_\chi}\right) + [|c_L^G|^2 - |c_R^G|^2] \mathcal{F}_S\left(\frac{m_{\chi^-}}{m_\chi}, \frac{m_V}{m_\chi}\right) \right\}, \quad (2.7)$$

where

$$\mathcal{F}_X(\mu, \eta) = \frac{3}{2} \log\left(\frac{\mu^2}{\eta^2}\right) + (3\eta^2 - 3\mu^2 + n_X) f(\mu, \eta), \quad (2.8)$$

for $X = V, S$, with $n_V = -7$, $n_S = 1$, and

$$f(\mu, \eta) = \begin{cases} \frac{1}{2\sqrt{\Delta}} \log \frac{\mu^2 + \eta^2 - 1 + \sqrt{\Delta}}{\mu^2 + \eta^2 - 1 - \sqrt{\Delta}} & \Delta \neq 0 \\ \frac{2}{(\mu^2 - \eta^2)^2 - 1} & \Delta = 0 \end{cases}, \quad (2.9)$$

with $\Delta \equiv \Delta(\mu, \eta) = (\mu^2 + \eta^2 - 1)^2 - 4\mu^2\eta^2$. Contour plots of $\mathcal{F}_V(\mu, \eta)$ and $\mathcal{F}_S(\mu, \eta)$ are shown in fig. 2, and present a discontinuity at $\mu^2 + \eta^2 = 1$. The anapole interaction, being P-violating, must vanish if the underlying model preserves parity, namely when $v_L = v_R$ and $c_L^G = c_R^G$, as apparent from Eq. (2.7).

¹We have used the Feynman rules for Majorana fermions derived in [54, 55]; the calculation was performed with the help of `FeynCalc` [56–58], `FeynHelpers` [59] and `Package-X` [60].

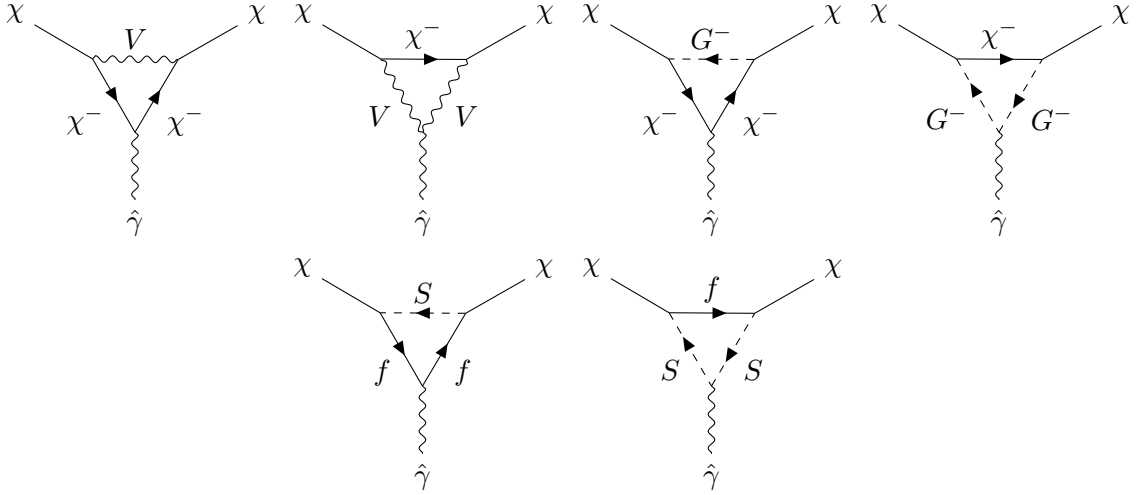


Figure 1: Feynman diagrams generating an anapole moment for a Majorana fermion at the one-loop level in the background field formulation, via the mediation of an electrically charged vector boson (top) or the mediation of a charged scalar (bottom).

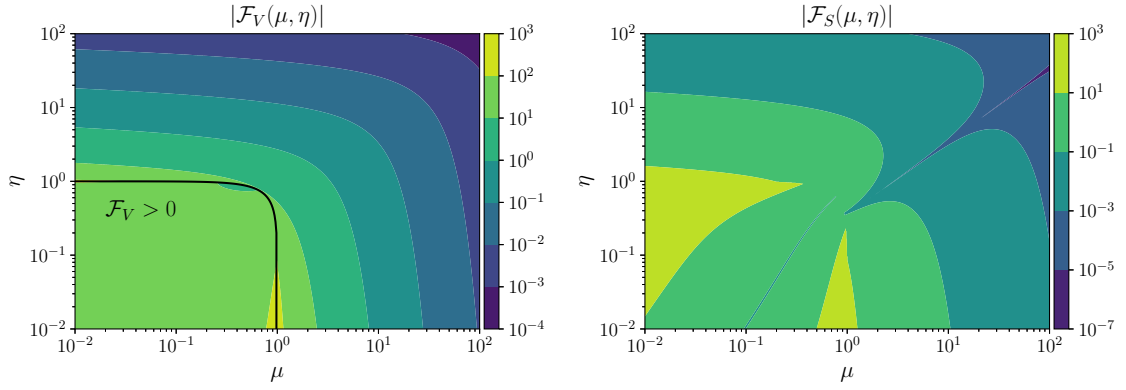


Figure 2: Absolute values of the functions $\mathcal{F}_V(\mu, \eta)$ (left) and $\mathcal{F}_S(\mu, \eta)$ (right).

We also consider the scenario where χ couples to a charged Dirac fermion f and a charged complex scalar S , with masses m_f and m_S , and with charges $\pm eQ_f$ respectively (see also [23, 28, 31, 33]). The interaction Lagrangian in this case can be written as

$$\mathcal{L}_{\text{FFS}} = \bar{\chi} [c_L P_L + c_R P_R] S^* f + \text{h.c.}, \quad (2.10)$$

allowing χ to interact with the (background) photon field via the diagrams shown in fig. 1. The induced scalar contribution to the anapole moment reads

$$\mathcal{A}_S = -\frac{e}{96\pi^2 m_\chi^2} Q_f \left[|c_L|^2 - |c_R|^2 \right] \mathcal{F}_S\left(\frac{m_f}{m_\chi}, \frac{m_S}{m_\chi}\right). \quad (2.11)$$

The resulting vector- and scalar contributions to the anapole moment of χ are shown in figs. 3 and 4 as a function of $\eta = m_{S,V}/m_\chi$, for different values of the fermion mass

m_{f,χ^-} . In both cases the anapole moment is enhanced for $\eta \approx 1$ and $m_{f,\chi^-} \ll m_\chi$. The dependence of the anapole moment with $\mu = m_{f,\chi^-}/m_\chi$ is similar, see also fig. 2.²

The general formulas eq. (2.7) and eq. (2.11) simplify when the charged fermions are much heavier than the vector/scalar and the Majorana fermion, *i.e.* when $m_{f,\chi^-} \gg m_{S,V}, m_\chi$. In this case, we find

$$\begin{aligned}\mathcal{A}_V &\simeq \frac{e}{96\pi^2 m_{\chi^-}^2} \left\{ 2 \left[|v_L|^2 - |v_R|^2 \right] \left(3 + 5 \log \frac{m_V^2}{m_{\chi^-}^2} \right) + \left[|c_L^G|^2 - |c_R^G|^2 \right] \left(3 + \log \frac{m_V^2}{m_{\chi^-}^2} \right) \right\}, \\ \mathcal{A}_S &\simeq -\frac{e}{96\pi^2 m_f^2} Q_f \left[|c_L|^2 - |c_R|^2 \right] \left(3 + \log \frac{m_S^2}{m_f^2} \right),\end{aligned}\quad (2.12)$$

which are independent of m_χ . Analogously, in the heavy scalar/vector limit, *i.e.* when $m_{V,S} \gg m_\chi, m_f$

$$\begin{aligned}\mathcal{A}_V &\simeq \frac{e}{96\pi^2 m_V^2} \left\{ 2 \left[|v_L|^2 - |v_R|^2 \right] \left(-3 + 2 \log \frac{m_{\chi^-}^2}{m_V^2} \right) - \left[|c_L^G|^2 - |c_R^G|^2 \right] \left(3 + 2 \log \frac{m_{\chi^-}^2}{m_V^2} \right) \right\}, \\ \mathcal{A}_S &\simeq \frac{e}{96\pi^2 m_S^2} Q_f \left[|c_L|^2 - |c_R|^2 \right] \left(3 + 2 \log \frac{m_f^2}{m_S^2} \right).\end{aligned}\quad (2.13)$$

This general formalism can be applied in particular to calculate the anapole moment of the Standard Model neutrinos, through its interactions with the W boson and the charged leptons. In this case, $v_L = g/\sqrt{2}$, $v_R = c_L^G = c_R^G = 0$, resulting in [46, 48]

$$\mathcal{A} \simeq \frac{e G_F}{12\sqrt{2}\pi^2} (-3 + 2 \log \frac{m_\ell^2}{m_W^2}), \quad (2.14)$$

where $G_F = \sqrt{2}g^2/8m_W^2$ is the Fermi constant, with m_W the W -boson mass, and m_ℓ is the charged lepton mass.

For Dirac fermions, the anapole moment is half as large as for Majorana fermions, due to the halving of the number of diagrams.

3 Anapole Moment of the Lightest Neutralino in the MSSM

An archetype of Majorana fermion interacting with charged particles both via a charged vector mediator and a charged scalar mediator is the lightest neutralino in the MSSM. The MSSM Lagrangian contains an interaction term between the lightest neutralino, the charginos χ_j , $j = 1, 2$, and the W -boson (and its Goldstone boson). This term has the form

$$\mathcal{L} \supset \bar{\chi} \gamma^\mu \left[v_L^j P_L + v_R^j P_R \right] \chi_j^- W_\mu^+ + \bar{\chi} \left[c_L^{G,j} P_L + c_R^{G,j} P_R \right] \chi_j^- G^+ + \text{h.c.}, \quad (3.1)$$

²The “compressed” spectrum requires a certain adjustment of the fundamental parameters of the model. On the other hand, it is a viable possibility from the phenomenological point of view, and has attracted some attention in the literature in the context of dark matter production via coannihilations [61, 62], indirect detection [63, 64], or collider searches [65, 66]. For an extensive review, see [28].

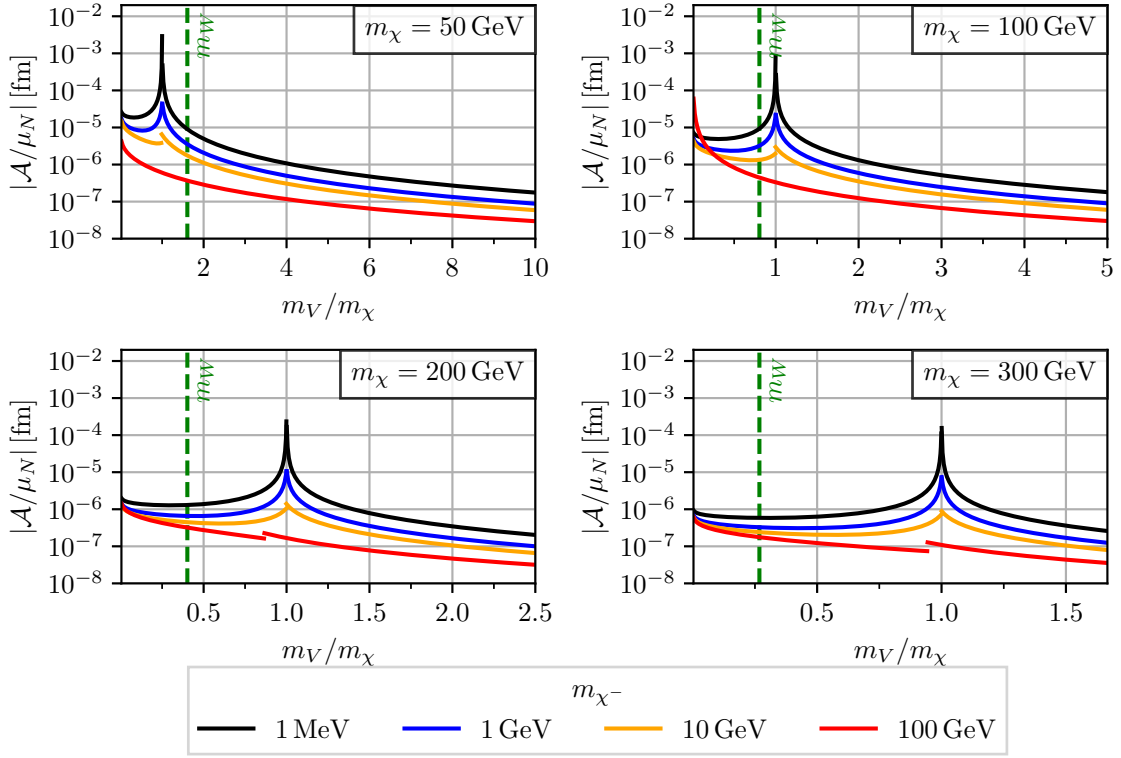


Figure 3: Anapole moment (normalized to the nuclear magneton μ_N) induced at the one loop level via the interaction of the Majorana fermion χ with a charged gauge boson V and a charged fermion χ^- , as a function of m_V/m_χ , for different values of the Majorana mass and different values of the charged fermion mass. For the plot, we assumed for concreteness $v_L = 1$ and $v_R, c_L^G, c_R^G = 0$.

with

$$\begin{aligned}
v_L^j &= -g N_{12} U_{j1}^* - g \frac{1}{\sqrt{2}} N_{13} U_{j2}^*, \\
v_R^j &= -g N_{12}^* V_{j1} + g \frac{1}{\sqrt{2}} N_{14}^* V_{j2}, \\
c_L^{G,j} &= g \cos \beta \left[N_{13}^* U_{j1}^* - \frac{1}{\sqrt{2}} U_{j2}^* (N_{12}^* + \tan \theta_W N_{11}^*) \right], \\
c_R^{G,j} &= -g \sin \beta \left[N_{14} V_{j1} + \frac{1}{\sqrt{2}} V_{j2} (N_{12} + \tan \theta_W N_{11}) \right],
\end{aligned} \tag{3.2}$$

where $\tan \beta = \langle H_2^0 \rangle / \langle H_1^0 \rangle$ denotes the ratio between the expectation values of the neutral components of the up-type Higgs and the down-type Higgs doublet, θ_W is the Weinberg's angle, N_{ij} , $i, j = 1, \dots, 4$ are the elements of the neutralino mixing matrix, and U_{ij} (V_{ij}), $i, j = 1, 2$ are the elements of the mixing matrix of the negatively (positively) charged chargino (see appendix A for a brief summary of the construction of the mass eigenstates in the MSSM from the interaction eigenstates).

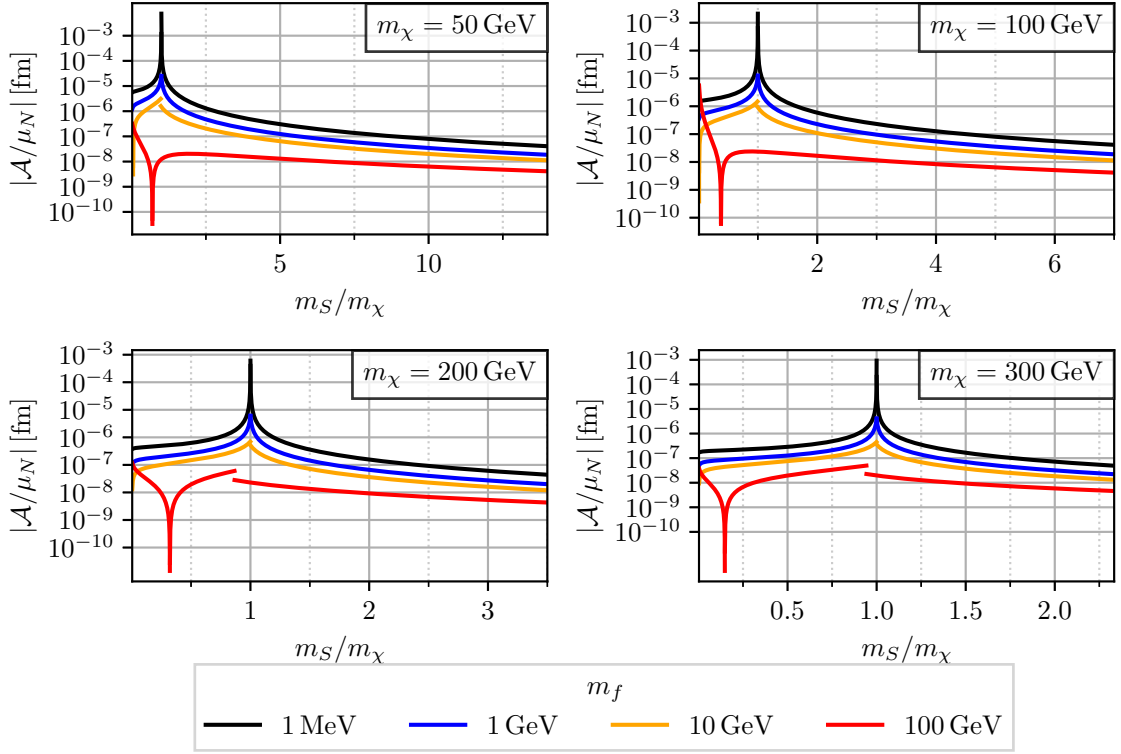


Figure 4: Same as Fig. 3 but for a Majorana fermion that interacts with a charged scalar S and a charged fermion f . For the plot, we assumed for concreteness $c_L = 1$, $c_R = 0$ and $Q_f = -1$.

Further, the Lagrangian contains an interaction term with the chargino and the charged Higgs, of the form

$$\mathcal{L}_{\text{FFS}} \supset \bar{\chi} \left[c_L^{H,j} P_L + c_R^{H,j} P_R \right] H^+ \chi_j^- + \text{h.c.}, \quad (3.3)$$

with

$$\begin{aligned} c_L^{H,j} &= -g \sin \beta \left[N_{13}^* U_{j1}^* - \frac{1}{\sqrt{2}} U_{j2}^* (N_{12}^* + \tan \theta_W N_{11}^*) \right], \\ c_R^{H,j} &= -g \cos \beta \left[N_{14} V_{j1} + \frac{1}{\sqrt{2}} V_{j2} (N_{12} + \tan \theta_W N_{11}) \right], \end{aligned} \quad (3.4)$$

as well as an interaction term with the SM fermions and sfermions of the form

$$\mathcal{L}_{\text{FFS}} \supset \bar{\chi} \left[c_L^{i,a} P_L + c_R^{i,a} P_R \right] \tilde{f}_a f_i + \text{h.c.}, \quad (3.5)$$

with

$$\begin{aligned} c_L^{i,1} &= G^{f_{iL}} \cos \theta_{\tilde{f}_a} + H^{f_{iR}} \sin \theta_{\tilde{f}_a}, \\ c_R^{i,1} &= G^{f_{iR}} \sin \theta_{\tilde{f}_a} + H^{f_{iL}} \cos \theta_{\tilde{f}_a}, \\ c_L^{i,2} &= -G^{f_{iL}} \sin \theta_{\tilde{f}_a} + H^{f_{iR}} \cos \theta_{\tilde{f}_a}, \\ c_R^{i,2} &= G^{f_{iR}} \cos \theta_{\tilde{f}_a} - H^{f_{iL}} \sin \theta_{\tilde{f}_a}, \end{aligned} \quad (3.6)$$

and

$$\begin{aligned}
G^{f_{iL}} &= -\sqrt{2}g \left[T_{3L}^{f_i} N_{12}^* + \tan \theta_W (Q_{f_i} - T_{3L}^{f_i}) N_{11}^* \right], \\
G^{f_{iR}} &= \sqrt{2}g \tan \theta_W Q_{f_i} N_{11}, \\
H^{f_{iL}} &= -\frac{g}{\sqrt{2}m_W} m_{f_i} \times \begin{cases} N_{14}/\sin \beta, & f_i = u\text{-type} \\ N_{13}/\cos \beta, & f_i = d\text{-type}, \ell \end{cases} \\
H^{f_{iR}} &= H^{f_{iL}*}.
\end{aligned} \tag{3.7}$$

These interactions induce at the one loop level an anapole moment for the lightest neutralino χ :

$$\mathcal{A} = \mathcal{A}_W + \mathcal{A}_{\tilde{f}} + \mathcal{A}_H. \tag{3.8}$$

Using the general results of section 2 for the vector and scalar contributions to the anapole moment of a Majorana fermion, one finds

$$\begin{aligned}
\mathcal{A}_W &= \frac{e}{96\pi^2 m_\chi^2} \left\{ 2 \sum_j \left[|v_L^j|^2 - |v_R^j|^2 \right] \mathcal{F}_W \left(\frac{m_{\chi_j^-}}{m_\chi}, \frac{m_{W^+}}{m_\chi} \right) \right. \\
&\quad \left. + \sum_j \left[|c_L^{G,j}|^2 - |c_R^{G,j}|^2 \right] \mathcal{F}_S \left(\frac{m_{\chi_j^-}}{m_\chi}, \frac{m_{W^+}}{m_\chi} \right) \right\}, \\
\mathcal{A}_{\tilde{f}} &= -\frac{e}{96\pi^2 m_\chi^2} \sum_{i,a} N_c^i Q_i \left[|c_L^{i,a}|^2 - |c_R^{i,a}|^2 \right] \mathcal{F}_S \left(\frac{m_{f_i}}{m_\chi}, \frac{m_{\tilde{f}_a}}{m_\chi} \right), \\
\mathcal{A}_H &= -\frac{e}{96\pi^2 m_\chi^2} \sum_j Q_j \left[|c_L^{H,j}|^2 - |c_R^{H,j}|^2 \right] \mathcal{F}_S \left(\frac{m_{\chi_j^-}}{m_\chi}, \frac{m_{H^+}}{m_\chi} \right).
\end{aligned} \tag{3.9}$$

In what follows, we will particularize these expressions to some well motivated MSSM scenarios.

4 MSSM Scenarios

In order to gain insight into the rich physics of supersymmetric models, we will study first in subsections 4.1, 4.2 and 4.3 some simplified scenarios where some SUSY particles are integrated out. Lastly, in subsection 4.4, we will consider a general MSSM scenario.

4.1 Pure lightest neutralino & heavy sfermions

Let us first consider a number of toy models where the lightest neutralino practically coincides with an interaction eigenstate, either the bino, the higgsino, or the wino. We also consider first that all sfermions are decoupled, so that $\mathcal{A}_{\tilde{f}} \simeq 0$.

Bino limit

In the limit $M_1 \ll M_2, |\mu|, m_{\tilde{f}}$, the lightest neutralino is practically inert and in particular does not couple to the W boson, so that $\mathcal{A}_W \simeq 0$, nor to the charged Higgs, so that $\mathcal{A}_H \simeq 0$. The anapole moment in this toy model is therefore expected to be very suppressed.

Higgsino limit

In the limit $|\mu| \ll M_1, M_2, m_{\tilde{f}}$ the two lightest neutralinos are nearly degenerate in mass and form a pseudo-Dirac pair. Further, there is only one light chargino, which practically coincides with the charged Higgsino. The effective couplings of the lightest neutralino to the W -boson and the lightest chargino read:

$$\begin{aligned} v_L^1 &\simeq -\frac{g}{2}, & v_R^1 &\simeq \frac{g}{2}, \\ c_L^{G,1} &\simeq 0, & c_R^{G,1} &\simeq 0. \end{aligned} \quad (4.1)$$

and are manifestly parity conserving. The vector contribution to the anapole moment is therefore suppressed in this scenario, $\mathcal{A}_W \simeq 0$. The same result holds for a minimal dark matter scenario where the dark matter particle is a Majorana fermion, doublet under $SU(2)_L$ and with hypercharge $1/2$.

In the MSSM, moreover, the lightest neutralino also couples to the chargino and to the charged Higgs, which may be light. On the other hand, it follows from eq. (3.4) that in the Higgsino limit the coupling strengths are $c_R^{H,1}, c_L^{H,1} \simeq 0$, and therefore $\mathcal{A}_H \simeq 0$ regardless of the mass of the charged Higgs.

Wino limit

In the limit $M_2 \ll M_1, |\mu|, m_{\tilde{f}}$, there is only one light neutralino and one light chargino, which are composed mainly by a neutral wino and a charged wino respectively. In this limit, the anapole moment only receives contributions from the chargino- W loop. The relevant coupling constants read

$$\begin{aligned} v_L^1 &= -g, & v_R^1 &= -g, \\ c_L^{G,1} &= 0, & c_R^{G,1} &= 0. \end{aligned} \quad (4.2)$$

which are manifestly parity conserving and lead to a suppressed anapole moment.

It is apparent from these limiting cases that in order to enhance the anapole moment it is necessary to couple the lightest neutralino to new light particles with parity breaking interactions, and/or to introduce an admixture in the neutralino eigenstate of different interaction eigenstates. We discuss these two possibilities below.

4.2 Light sfermion scenarios

In this subsection we revisit the scenarios considered above, but allowing for a contribution to the anapole moment from fermion-sfermion loops.

Bino limit

As discussed in subsection 4.1, in the limit of heavy sfermions, the lightest neutralino does not couple to the W boson nor to the charged Higgs, therefore $\mathcal{A}_W, \mathcal{A}_H \simeq 0$. On the other hand, the bino couples to the Standard Model fermions and sfermions, and the sfermions in the loop could contribute sizably to the anapole moment if they are sufficiently light. We consider here a simplified scenario where the bino couples to the left- and right-handed

components of a Standard Model fermion f (with color charge N_c , electric charge Q_f and isospin T_{3L}^f), and the sfermions \tilde{f}_L and \tilde{f}_R . We denote the two scalar mass eigenstates as \tilde{f}_1 and \tilde{f}_2 , which are obtained from the interaction eigenstates \tilde{f}_L and \tilde{f}_R by rotating by the angle $\theta_{\tilde{f}}$ (see Appendix A). The strength of the Yukawa coupling of the lightest neutralino to the sfermion mass eigenstates \tilde{f}_1 and \tilde{f}_2 and the left- and right-handed components of the Standard Model fermion f explicitly read:

$$\begin{aligned} c_L^1 &= -\sqrt{2}g \left[\tan \theta_W (Q_f - T_{3L}^f) \right] \cos \theta_{\tilde{f}}, & c_R^1 &= \sqrt{2}g \tan \theta_W Q_f \sin \theta_{\tilde{f}}, \\ c_L^2 &= \sqrt{2}g \left[\tan \theta_W (Q_f - T_{3L}^f) \right] \sin \theta_{\tilde{f}}, & c_R^2 &= \sqrt{2}g \tan \theta_W Q_f \cos \theta_{\tilde{f}}, \end{aligned} \quad (4.3)$$

which are in general parity violating and therefore will generate a non-vanishing contribution to the anapole moment.

We show in the top left panel of fig. 5 a scatter plot of the expected anapole moment (normalized to the nuclear magneton) for the pure bino scenario for $m_\chi \in [10^1, 10^4]$ GeV, $m_{\tilde{f}_1} \in [m_\chi, 10m_\chi]$, $m_{\tilde{f}_2} \in [m_{\tilde{f}_1}, 10m_\chi]$, and $\theta_{\tilde{f}} \in [0, 2\pi]$. In the plot we have taken for concreteness $m_f = m_\tau = 1.7$ GeV, and we have imposed the constraints on the stau mass from ATLAS [67] and from the LEP experiments [68]. Generically, one finds $|\mathcal{A}|/\mu_N \sim 10^{-8}(m_\chi/100 \text{ GeV})^{-2} \text{ fm}$, although there are a few points with $10^{-6} \text{ fm} \lesssim |\mathcal{A}|/\mu_N \lesssim 10^{-5} \text{ fm}$ for $m_\chi \lesssim 100 \text{ GeV}$ where the anapole moment is enhanced, corresponding to a compressed spectrum scenario where the stau mass is close to the bino mass.

Higgsino limit

In order to generate an anapole moment in this simplified scenario it is also necessary to introduce new light degrees of freedom with parity violating couplings. As for the bino limit analyzed above, we consider the scenario where the Higgsino couples to the left- and right-handed components of a Standard Model fermion f and the sfermions \tilde{f}_L and \tilde{f}_R , with mass eigenstates \tilde{f}_1 and \tilde{f}_2 . The coupling strengths to the mass eigenstates explicitly read:

$$\begin{aligned} c_L^1 &= H^{fL} \sin \theta_{\tilde{f}}, & c_R^1 &= H^{fL} \cos \theta_{\tilde{f}}, \\ c_L^2 &= H^{fL} \cos \theta_{\tilde{f}}, & c_R^2 &= -H^{fL} \sin \theta_{\tilde{f}}, \end{aligned} \quad (4.4)$$

with

$$H^{fL} = -\frac{g}{2m_W} m_f \times \begin{cases} 1/\sin \beta, & f = u\text{-type} \\ 1/\cos \beta, & f = d\text{-type}, \ell \end{cases}, \quad (4.5)$$

which are as before parity violating.

We show in the top right panel of fig. 5 a scatter plot of the anapole moment for the pure higgsino scenario, for the same range of parameters as for the pure bino scenario, and taking $\tan \beta = 5$ (red points) or $\tan \beta = 50$ (blue points). Clearly the anapole moment increases with $\tan \beta$, as the Higgsino coupling to the tau-stau grows with $\cos^{-2} \beta$.

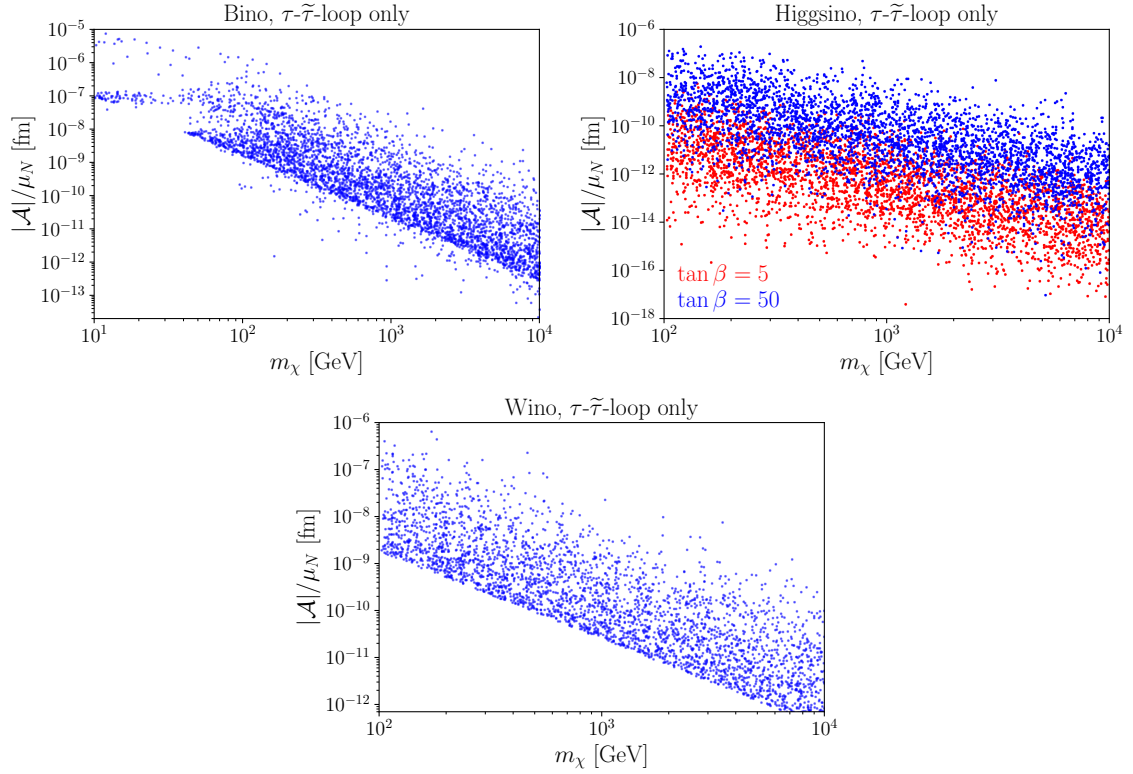


Figure 5: Anapole moment (normalized to the nucleon magneton) for simplified MSSM scenarios with pure bino (top left), pure higgsino (top right), and pure wino (bottom) lightest neutralino, coupling only with the tau and staus. For details, see subsection 4.2.

Wino limit

Similarly to the previous two scenarios, in the wino limit the anapole moment can only be generated by parity-violating interactions of the lightest neutralino with fermions and sfermions. The coupling strengths to the sfermion mass eigenstates \tilde{f}_1 and \tilde{f}_2 read in this limit:

$$\begin{aligned} c_L^{i,1} &= -\sqrt{2}gT_{3L}^{f_i} \cos \theta_{\tilde{f}}, & c_R^{i,1} &= 0, \\ c_L^{i,2} &= \sqrt{2}gT_{3L}^{f_i} \sin \theta_{\tilde{f}}, & c_R^{i,2} &= 0, \end{aligned} \quad (4.6)$$

which are clearly parity violating.

The expected anapole moment in this scenario is shown in the lower panel of fig. 5, for the same ranges of parameters as for the Bino limit.

4.3 Mixed lightest neutralino & decoupled sfermions

Finally, we consider a simplified scenario where the sfermions are very heavy, so that $\mathcal{A}_{\tilde{f}} \simeq 0$, but with an admixture of interaction eigenstates in the lightest neutralino mass eigenstates, which may allow parity violating interactions.

Mixed Bino-Higgsino

In the limit $M_1, \mu \ll M_2$, there is only one light chargino, which is purely a charged Higgsino. The couplings of the lightest neutralino to the charged Higgsino and the W are:

$$\begin{aligned} v_L^1 &= -g \frac{1}{\sqrt{2}} N_{13}, & v_R^1 &= +g \frac{1}{\sqrt{2}} N_{14}^*, \\ c_L^{G,1} &= -\frac{g}{\sqrt{2}} \cos \beta \tan \theta_W N_{11}^*, & c_R^{G,1} &= -\frac{g}{\sqrt{2}} \sin \beta \tan \theta_W N_{11}, \end{aligned} \quad (4.7)$$

which are in general parity violating, thus leading to a non-zero \mathcal{A}_W . The couplings to the chargino and the charged Higgs read

$$c_L^{H,1} = g \sin \beta \tan \theta_W N_{11}^*, \quad c_R^{H,1} = -g \cos \beta \tan \theta_W N_{11}, \quad (4.8)$$

which are also in general parity violating and can further increase the anapole moment.

We show in the left panel in fig. 6 the expected anapole moments for this scenario, taking for concreteness $M_1, \mu \in [100, 10^5] \text{ GeV}$ and $\tan \beta = 5$. We assume for simplicity that the charged Higgs is very heavy and does not contribute to the anapole moment (although clearly for a light charged Higgs the anapole moment could be enhanced). In the plot we also indicate whether the lightest neutralino is bino like ($|N_{11}| > 0.95$), higgsino like ($\sqrt{N_{13}^2 + N_{14}^2} > 0.95$) or a mixed state. As expected, the anapole moment is enhanced when the lightest neutralino is not a pure state, but an admixture of bino and higgsino.

Mixed Bino-Wino

In the limit $M_1, M_2 \ll \mu$, there is only one light chargino, which is purely a charged wino. The couplings of the lightest neutralino to the charged Higgsino and the W are:

$$\begin{aligned} v_L^1 &= -g N_{12}, & v_R^1 &= -g N_{12}^*, \\ c_L^{G,1} &= 0, & c_R^{G,1} &= 0, \end{aligned} \quad (4.9)$$

which preserve parity and therefore give $\mathcal{A}_W \simeq 0$. Further, the couplings to the chargino and the charged Higgs are:

$$c_L^{H,1} = 0, \quad c_R^{H,1} = 0. \quad (4.10)$$

Therefore, also in the scenario where the lightest neutralino is a mixed bino-wino state, only the sfermion loops can generate a non-vanishing anapole moment.

Mixed Wino-Higgsino

In the limit $M_2, \mu \ll M_1$ both charginos can be light and contribute to the anapole moment via the interactions with the W and with the charged Higgs boson. The coupling strengths

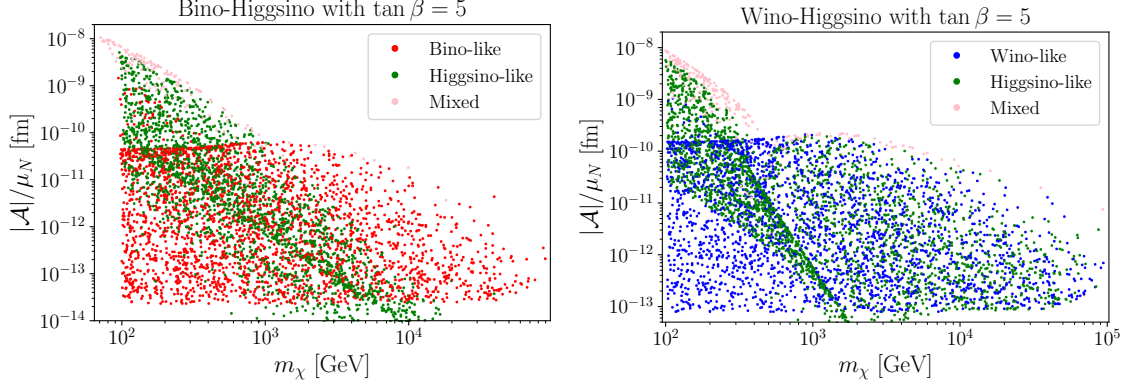


Figure 6: Anapole moment (normalized to the nucleon magneton) for simplified MSSM scenarios with mixed bino-higgsino (left) and wino-higgsino (right) lightest neutralino. For details, see subsection 4.3.

of the lightest neutralino to the charginos χ_i^\pm , $i = 1, 2$ and the W boson read:

$$\begin{aligned}
v_L^j &= -g N_{12} U_{j1}^* - g \frac{1}{\sqrt{2}} N_{13} U_{j2}^*, \\
v_R^j &= -g N_{12}^* V_{j1} + g \frac{1}{\sqrt{2}} N_{14}^* V_{j2}, \\
c_L^{G,j} &= g \cos \beta \left[N_{13}^* U_{j1}^* - \frac{1}{\sqrt{2}} U_{j2}^* (N_{12}^*) \right], \\
c_R^{G,j} &= -g \sin \beta \left[N_{14} V_{j1} + \frac{1}{\sqrt{2}} V_{j2} (N_{12}) \right],
\end{aligned} \tag{4.11}$$

while for the charged Higgs boson,

$$\begin{aligned}
c_L^{H,j} &= -g \sin \beta \left[N_{13}^* U_{j1}^* - \frac{1}{\sqrt{2}} U_{j2}^* (N_{12}^*) \right], \\
c_R^{H,j} &= -g \cos \beta \left[N_{14} V_{j1} + \frac{1}{\sqrt{2}} V_{j2} (N_{12}) \right].
\end{aligned} \tag{4.12}$$

These interactions are in general parity violating and lead to a non-vanishing anapole moment. A numerical scan of this scenario is shown in the right panel in fig. 6, for the same set-up as in the bino-higgsino mixed case; the conclusions in the wino-higgsino case are also analogous to that case.

4.4 General MSSM scenarios

So far we have concentrated in some limiting scenarios where most SUSY particles are assumed to be very heavy and integrated-out. On the other hand, in generic scenarios several SUSY particles can be light and can contribute sizeable to the anapole moment. To estimate the anapole moment expected in a generic SUSY scenario, we will consider in this subsection MSSM scenarios defined by the ranges indicated in table 1 (at the scale $\Lambda = 3$ TeV).

Parameter	Range
M_1	[100, 2000] GeV
M_2	[100, 2000] GeV
M_3	[2000, 5000] GeV
$A_{t,b,\tau}$	[-4000, 4000] GeV
m_A	$[10^3, 10^5]$ GeV
$\tan\beta$	[3, 50]
μ	[100, 2000] GeV
$m_{\tilde{\ell}_{L,R}}$	[100, 2000] GeV
$m_{\tilde{q}_{L1,2}}$	[400, 2000] GeV
$m_{\tilde{u}_{R1,2}}, m_{\tilde{d}_{R1,2}}$	[400, 2000] GeV
$m_{\tilde{q}_{L3}}$	[300, 2000] GeV
$m_{\tilde{u}_{R3}}, m_{\tilde{d}_{R3}}$	[300, 2000] GeV

Table 1: Ranges of parameters, defined at the scale $\Lambda = 3$ TeV, for the MSSM scan described in subsection 4.4.

From those boundary conditions, we generate the low energy spectrum using **SOFTSUSY4.0** [69]. We then select the points satisfying the LEP constraints (using **micrOMEGAs v3** [70]), and ATLAS and CMS constraints (using **SModelS v2** [71]), leading to a Higgs boson with mass in the range 123-127 GeV (using **HiggsBounds v4** [72] and **HiggsSignals** [73]), and satisfying various flavor physics constraints (using **SuperIso v3.0** [74] and **GM2Calc** [75]).³ These points do not necessarily reproduce the observed dark matter abundance in the standard freeze-out mechanism, although they could become viable for other production mechanisms. Since we are interested in the generic size of the neutralino anapole moment, we will disregard in our analysis the constraints from Cosmology. The resulting values of the anapole moment, calculated using the general expressions from section 3, are shown in fig. 7.

We find points where the anapole moment can reach values up to $|\mathcal{A}|/\mu_N \sim 10^{-6}$ fm. These correspond to scenarios where the anapole moment is dominated by the fermion-sfermion contribution and where the LSP and a sfermion are almost mass-degenerate, in accordance with the results for the simplified models of section 4.2 (with $\mathcal{O}(1)$ enhancements when several sfermions circulate in the loop), and correspond to scenarios where the lightest neutralino contains a significant bino and/or wino component. For scenarios where the lightest neutralino is Higgsino like, the anapole moment is typically more suppressed.

³We used **PySLHA** [76] for linking the various codes via the **SLHA** [77] format.

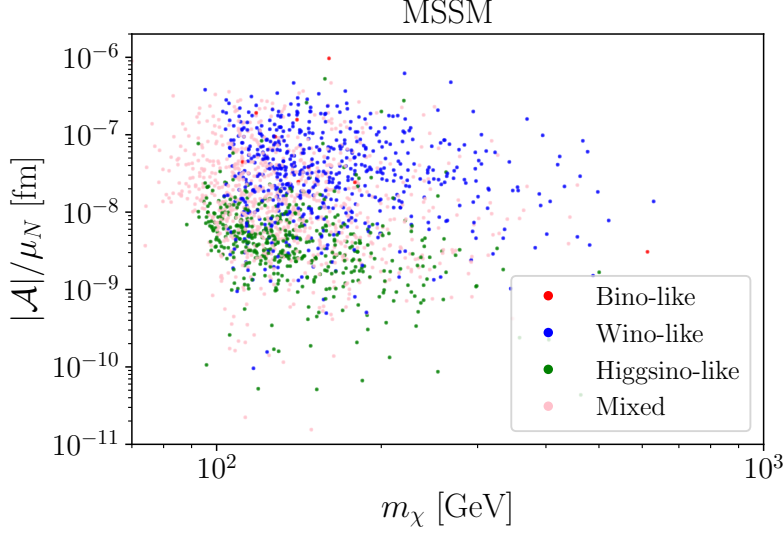


Figure 7: Anapole moment for MSSM scenarios with parameters in the ranges listed in Table 1 and satisfying the experimental constraints discussed in subsection 4.4.

5 Direct Dark Matter Detection Through the Anapole Moment

The effective Lagrangian eq. (2.2) gives rise to a dark matter interaction with the nuclei, that can induce an observable signal in direct detection experiments.⁴ The differential scattering cross section induced by the interaction of the Majorana dark matter particle with a target nucleus via the anapole moment reads [21, 27]:

$$\frac{d\sigma}{dE_R} = \alpha_{\text{EM}} \mathcal{A}^2 \left[Z^2 \left(2m_T - \left(1 + \frac{m_T}{m_\chi} \right) \frac{E_R}{v^2} \right) F_Z^2(q^2) + \frac{1}{3} \frac{m_T}{m_\chi^2} \left(\frac{\bar{\mu}_T}{\mu_N} \right)^2 \frac{E_R}{v^2} F_D^2(q^2) \right], \quad (5.1)$$

where m_T and Z are the nucleus mass and electric charge, E_R is the recoil energy (related to the momentum transfer through $q^2 = 2m_TE_R$) and v is the dark matter speed relative to the nucleus. Further, F_Z and F_D are the charge and magnetic dipole moment form factors [78, 79]:

$$F_Z^2(q^2) = \left(\frac{3j_1(qR)}{qR} \right)^2 e^{-q^2 s^2}, \quad (5.2)$$

$$F_D^2(q^2) = \begin{cases} \left[\frac{\sin(qR_D)}{qR_D} \right]^2 & (qR_D < 2.55, qR_D > 4.5) \\ 0.047 & (2.55 \leq qR_D \leq 4.5) \end{cases}. \quad (5.3)$$

where $j_1(x)$ is a spherical Bessel function of the first kind, $R = \sqrt{c^2 + \frac{7}{3}\pi^2 a^2 - 5s^2}$ (with $c = (1.23A^{1/3} - 0.60)$ fm, $a = 0.52$ fm and $s = 0.9$ fm) and $R_D \simeq 1.0A^{1/3}$ fm. A denotes the

⁴More strictly, the contact interaction approximation holds when the momentum transfer is smaller than the masses in the loop, which we assume here. For coupling to electrons, a momentum-dependent form factor should instead be considered [23].

mass number of target nuclei. Further, $\mu_N = e/2m_p$ denotes the nuclear magneton, and $\bar{\mu}_T$ is the weighted dipole moment for the target nuclei, defined as:

$$\bar{\mu}_T = \left(\sum_i f_i \mu_i^2 \frac{S_i + 1}{S_i} \right)^{1/2}, \quad (5.4)$$

where f_i , μ_i , and S_i are the elemental abundance, nuclear magnetic moment, and spin, respectively, of the isotope i [18].

The differential event rate at a direct detection experiment reads:

$$\frac{dR}{dE_R} = \frac{1}{m_T} \frac{\rho_{\text{loc}}}{m_\chi} \int d^3v v f_{\text{Lab}}(\vec{v}) \frac{d\sigma}{dE_R}, \quad (5.5)$$

where $\rho_{\text{loc}} = 0.3 \text{ GeV cm}^{-3}$ and $f_{\text{Lab}}(\vec{v})$ denotes the dark matter velocity distribution in the laboratory frame. For the latter, we will adopt a Maxwell-Boltzmann distribution in the galactic frame, truncated at the escape velocity from the Galaxy, v_{esc} :

$$f_{\text{Lab}}(\vec{v}) = f(\vec{v} + \vec{v}_E), \quad (5.6)$$

with \vec{v}_E the velocity of the Earth in the galactic frame and

$$f(\vec{v}) = \begin{cases} \frac{1}{\mathcal{N}} e^{-v^2/v_0^2} & (|\vec{v}| < v_{\text{esc}}) \\ 0 & (|\vec{v}| > v_{\text{esc}}) \end{cases}, \quad (5.7)$$

with

$$\mathcal{N} = \pi^{3/2} v_0^3 \left[\text{erf}\left(\frac{v_{\text{esc}}}{v_0}\right) - \frac{2v_{\text{esc}}}{\sqrt{\pi}v_0} e^{-\frac{v_{\text{esc}}^2}{v_0^2}} \right]. \quad (5.8)$$

Hereafter we take $v_{\text{esc}} = 544 \text{ km s}^{-1}$, $v_0 = 220 \text{ km s}^{-1}$ and $v_E = 232 \text{ km s}^{-1}$. Finally, we calculate the number of events at a given direct detection experiment integrating dR/dE_R over the recoil energy, taking into account the corresponding detection efficiency.

We show in fig. 8 the 90% C.L. upper limits on the anapole moment \mathcal{A} normalized by the nuclear magneton μ_N from the non-observation of a dark matter signal at the XENON1T [80], SuperCDMS [81], and CRESST-III [82] experiments, alongside with the expected sensitivity of the XENONnT experiment [83].⁵ We find that the current sensitivity from the XENON experiment reaches $\mathcal{A}/\mu_N \sim 10^{-5} \text{ fm}$ at $m_{\text{DM}} \sim 30 \text{ GeV}$, which is about one order of magnitude larger than the maximum anapole moment we predict for generic MSSM scenarios. For these scenarios, it would be necessary to improve in sensitivity by at least one order of magnitude in order to probe the anapole moment of a spin 1/2 Majorana dark matter candidate, unless the Earth is immersed in a region of the galaxy with an overdensity of dark matter. Let us note that for special choices of parameters, namely when the dark matter candidate is almost degenerate in mass with the scalar (or vector) in the loop and when the fermion is very light, the anapole moment is enhanced (*cf.* Figs. 3 and 4, and also [28]). In these very special cases, a signal might be expected.

⁵Details of the estimation of the detection efficiency are given in Appendix B of Ref. [26].

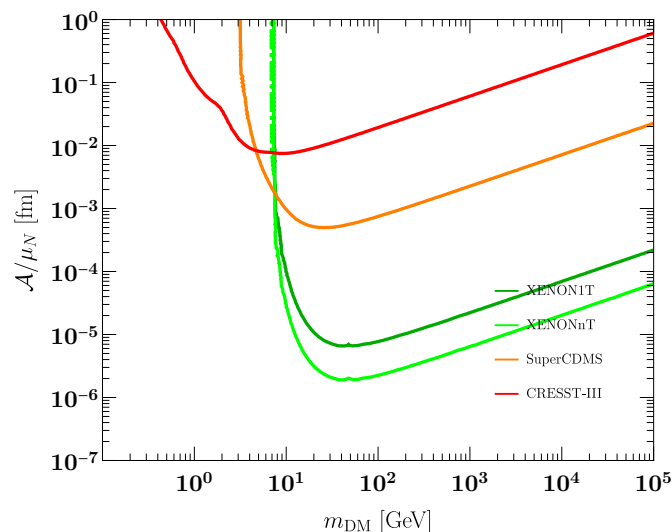


Figure 8: Upper limit on the anapole moment of a Majorana spin 1/2 fermion as dark matter candidate from the XENON1T, SuperCDMS and CRESST-III data, and projected sensitivity for XENONnT.

In this section we have considered simplified scenarios where the dark matter only interacts with the nucleon via the anapole moment. Clearly, there could be MSSM scenarios where the scattering mediated by squarks or by Higgses dominate over the one mediated by the anapole moment. For those scenarios, the discovery potential of dark matter accordingly increases. However, establishing the existence of an electromagnetic multiple moment for Majorana dark matter will become even more challenging.

6 Conclusions

In this work we have calculated the leading contribution to the anapole moment of a spin 1/2 Majorana fermion that interacts via a Yukawa or a gauge interaction with electromagnetically charged particles. To ensure the finiteness and the gauge independence of the vector contribution, we employed the background field method.

We have applied our general results to calculate the anapole moment of the lightest neutralino in the Minimal Supersymmetric Standard Model. Since the anapole interaction violates parity, only those MSSM scenarios violating parity will generate a non-vanishing anapole moment. We have also studied various limits where many supersymmetric particles are integrated out, and which can be identified with simplified dark matter models where the dark matter candidate is a Majorana fermion, that transforms as a singlet, doublet or triplet of $SU(2)_L$, and which could interact with a fermion and a sfermion via a Yukawa coupling.

Lastly, we have derived upper limits on the anapole moment of a Majorana fermion as dark matter candidate, from the null search results of direct detection experiments. For the parameters of the Standard Halo Model, we find that an improvement of sensitivity

of current experiments by at least one order of magnitude would be necessary in order to probe the anapole moment of generic dark matter scenarios.

Acknowledgments

The work of A.I. and M.R. was supported by the Collaborative Research Center SFB1258 and by the Deutsche Forschungsgemeinschaft (DFG, German Research Foundation) under Germany's Excellence Strategy - EXC-2094 - 390783311. The Feynman diagrams in this paper were drawn with the help of TikZ-Feynman [84].

A Particle Spectrum of the MSSM

In this Appendix we summarize the calculation of the particle mass eigenstates in terms of the interaction eigenstates in the Minimal Supersymmetric Standard Model (for reviews, see *e.g.* [85, 86]).

The R-parity odd neutral fermions of the MSSM are the bino (\tilde{B}), the neutral wino (\tilde{W}^0) and the two neutral Higgsinos (\tilde{H}_1^0 and \tilde{H}_2^0), with mass terms that can be cast as:

$$-\mathcal{L} = \frac{1}{2} \begin{pmatrix} \tilde{B} & \tilde{W}^0 & \tilde{H}_1^0 & \tilde{H}_2^0 \end{pmatrix} \mathcal{M}^n \begin{pmatrix} \tilde{B} \\ \tilde{W}^0 \\ \tilde{H}_1^0 \\ \tilde{H}_2^0 \end{pmatrix} + h.c., \quad (\text{A.1})$$

where \mathcal{M}^n is given by

$$\mathcal{M}^n = \begin{pmatrix} M_1 & 0 & -m_Z \sin \theta_W \cos \beta & m_Z \sin \theta_W \sin \beta \\ 0 & M_2 & m_Z \cos \theta_W \cos \beta & -m_Z \cos \theta_W \sin \beta \\ -m_Z \sin \theta_W \cos \beta & m_Z \cos \theta_W \cos \beta & 0 & -\mu \\ m_Z \sin \theta_W \sin \beta & -m_Z \cos \theta_W \sin \beta & -\mu & 0 \end{pmatrix}. \quad (\text{A.2})$$

Here, M_1 and M_2 are respectively the bino and wino masses, μ is the Higgsino mass parameter, θ_W is the weak mixing angle, and $\tan \beta \equiv \langle H_2^0 \rangle / \langle H_1^0 \rangle$ is the ratio of Higgs vacuum expectation values. The neutralinos χ_i , $i = 1, 2, 3, 4$ are defined as the R-parity-odd neutral fermion mass eigenstates, and are constructed by diagonalizing the mass matrix \mathcal{M}^n . To this end, one introduces the unitary matrix N , defined such that

$$N^* \mathcal{M}^n N^\dagger = \text{diag} (m_{\chi_1}, m_{\chi_2}, m_{\chi_3}, m_{\chi_4}) , \quad (\text{A.3})$$

with m_{χ_i} the neutralino masses, defined as real and positive, and ordered so that $m_{\chi_1} \leq m_{\chi_2} \leq m_{\chi_3} \leq m_{\chi_4}$. The neutralino states are related to the interaction eigenstates through:

$$\begin{pmatrix} \chi_1 \\ \chi_2 \\ \chi_3 \\ \chi_4 \end{pmatrix} = N \begin{pmatrix} \tilde{B} \\ \tilde{W}^0 \\ \tilde{H}_1^0 \\ \tilde{H}_2^0 \end{pmatrix}. \quad (\text{A.4})$$

Similarly, the R-parity odd charged fermions of the MSSM are the charged winos (\widetilde{W}^\pm) and the two charged Higgsinos (\widetilde{H}_1^- and \widetilde{H}_2^+). Their mass terms have the form:

$$-\mathcal{L} = \begin{pmatrix} \widetilde{W}^+ & \widetilde{H}_2^+ \end{pmatrix} \mathcal{M}^c \begin{pmatrix} \widetilde{W}^- \\ \widetilde{H}_1^- \end{pmatrix} + h.c., \quad (\text{A.5})$$

where

$$\mathcal{M}^c = \begin{pmatrix} M_2 & \sqrt{2}m_W \cos \beta \\ \sqrt{2}m_W \sin \beta & \mu \end{pmatrix}. \quad (\text{A.6})$$

with m_W the W-boson mass. The charginos χ_i^\pm , $i = 1, 2$ are defined as the R-parity odd charged fermion mass eigenstates, and are constructed from diagonalizing the mass matrix as

$$V \mathcal{M}^c U^T = \text{diag} \left(m_{\chi_1^-}, m_{\chi_2^-} \right), \quad (\text{A.7})$$

with $m_{\chi_1^-} \leq m_{\chi_2^-}$ and $m_{\chi_i^-}$ being real and positive. The charginos are related to the interaction eigenstates through:

$$\begin{pmatrix} \chi_1^- \\ \chi_2^- \end{pmatrix} = U \begin{pmatrix} \widetilde{W}^- \\ \widetilde{H}_1^- \end{pmatrix}, \quad \begin{pmatrix} \chi_1^+ \\ \chi_2^+ \end{pmatrix} = V \begin{pmatrix} \widetilde{W}^+ \\ \widetilde{H}_2^+ \end{pmatrix}, \quad (\text{A.8})$$

where U and V can be parameterized as

$$U = \begin{pmatrix} \cos \phi_L & \sin \phi_L \\ -\sin \phi_L & \cos \phi_L \end{pmatrix}, \quad V = \begin{pmatrix} \cos \phi_R & \sin \phi_R \\ -\epsilon_R \sin \phi_R & \epsilon_R \cos \phi_R \end{pmatrix}. \quad (\text{A.9})$$

with

$$\tan 2\phi_L = \frac{2\sqrt{2}m_W(\mu \sin \beta + M_2 \cos \beta)}{M_2^2 - \mu^2 - 2m_W^2 \cos 2\beta}, \quad (\text{A.10})$$

$$\tan 2\phi_R = \frac{2\sqrt{2}m_W(\mu \cos \beta + M_2 \sin \beta)}{M_2^2 - \mu^2 + 2m_W^2 \cos 2\beta}, \quad (\text{A.11})$$

$$\epsilon_R = \text{sgn} \left(M_2 \mu - m_W^2 \sin 2\beta \right). \quad (\text{A.12})$$

Finally, we focus on the sfermion mass term. The mass matrix for the superpartners of the SM fermion f reads:

$$-\mathcal{L} = \begin{pmatrix} \widetilde{f}_L^* & \widetilde{f}_R^* \end{pmatrix} \widetilde{\mathcal{M}}_f^2 \begin{pmatrix} \widetilde{f}_L \\ \widetilde{f}_R \end{pmatrix} + h.c., \quad (\text{A.13})$$

where

$$\widetilde{\mathcal{M}}_f^2 = \begin{pmatrix} \mathcal{M}_{fLL}^2 & \mathcal{M}_{fLR}^2 \\ (\mathcal{M}_{fLR}^2)^* & \mathcal{M}_{fRR}^2 \end{pmatrix}, \quad (\text{A.14})$$

with

$$\mathcal{M}_{fLL}^2 = m_{\tilde{f}_L}^2 + m_f^2 + m_Z^2 \cos 2\beta (T_{3f} - Q_f \sin^2 \theta_W), \quad (\text{A.15})$$

$$\mathcal{M}_{fRR}^2 = m_{\tilde{f}_R}^2 + m_f^2 + m_Z^2 \cos 2\beta Q_f \sin^2 \theta_W, \quad (\text{A.16})$$

$$\mathcal{M}_{fLR}^2 = \begin{cases} m_u(A_u - \mu \cot \beta) & \text{for } f = u \text{ (up-type quark)} \\ m_f(A_f + \mu \tan \beta) & \text{for } f = d, l \text{ (down-type quark, lepton)} \end{cases}. \quad (\text{A.17})$$

Here T_{3f} and Q_f are respectively the third component of isospin and the electric charge of the fermion f , $m_{\tilde{f}_L}^2$ and $m_{\tilde{f}_R}^2$ are soft SUSY breaking masses for the left- and right-handed chiral superfields, and A_f are soft SUSY breaking trilinear terms. The mass matrix can be diagonalized as

$$O_f \widetilde{\mathcal{M}}_f^2 O_f^T = \text{diag} \left(m_{\tilde{f}_1}^2, m_{\tilde{f}_2}^2 \right), \quad (\text{A.18})$$

with $m_{\tilde{f}_1}^2 \leq m_{\tilde{f}_2}^2$ and $m_{\tilde{f}_1}^2$ being real and positive. The sfermion mass eigenstates are related to the interaction eigenstates through:

$$\begin{pmatrix} \tilde{f}_1 \\ \tilde{f}_2 \end{pmatrix} = \begin{pmatrix} \cos \theta_f & \sin \theta_f \\ -\sin \theta_f & \cos \theta_f \end{pmatrix} \begin{pmatrix} \tilde{f}_L \\ \tilde{f}_R \end{pmatrix}. \quad (\text{A.19})$$

References

- [1] G. Jungman, M. Kamionkowski and K. Griest, *Supersymmetric dark matter*, [*Phys. Rept.* **267** \(1996\) 195](#) [[hep-ph/9506380](#)].
- [2] G. Bertone, D. Hooper and J. Silk, *Particle dark matter: Evidence, candidates and constraints*, [*Phys. Rept.* **405** \(2005\) 279](#) [[hep-ph/0404175](#)].
- [3] L. Bergström, *Nonbaryonic dark matter: Observational evidence and detection methods*, [*Rept. Prog. Phys.* **63** \(2000\) 793](#) [[hep-ph/0002126](#)].
- [4] J. L. Feng, *Dark Matter Candidates from Particle Physics and Methods of Detection*, [*Ann. Rev. Astron. Astrophys.* **48** \(2010\) 495](#) [[1003.0904](#)].
- [5] K. Fujikawa and R. Shrock, *The Magnetic Moment of a Massive Neutrino and Neutrino Spin Rotation*, [*Phys. Rev. Lett.* **45** \(1980\) 963](#).
- [6] S. T. Petcov, *The Processes $\mu \rightarrow e + \gamma$, $\mu \rightarrow e + \bar{e}, \nu' \rightarrow \nu + \gamma$ in the Weinberg-Salam Model with Neutrino Mixing*, [*Sov. J. Nucl. Phys.* **25** \(1977\) 340](#).
- [7] P. B. Pal and L. Wolfenstein, *Radiative Decays of Massive Neutrinos*, [*Phys. Rev. D* **25** \(1982\) 766](#).
- [8] R. E. Shrock, *Electromagnetic Properties and Decays of Dirac and Majorana Neutrinos in a General Class of Gauge Theories*, [*Nucl. Phys. B* **206** \(1982\) 359](#).
- [9] C. Giunti and A. Studenikin, *Neutrino electromagnetic properties*, [*Phys. Atom. Nucl.* **72** \(2009\) 2089](#) [[0812.3646](#)].
- [10] J. F. Nieves, *Electromagnetic Properties of Majorana Neutrinos*, [*Phys. Rev. D* **26** \(1982\) 3152](#).

- [11] B. Kayser, *Majorana Neutrinos and their Electromagnetic Properties*, *Phys. Rev. D* **26** (1982) 1662.
- [12] H. Aronson, *Spin-1 electrodynamics with an electric quadrupole moment*, *Phys. Rev.* **186** (1969) 1434.
- [13] K. J. F. Gaemers and G. J. Gounaris, *Polarization Amplitudes for $e^+ e^- \rightarrow W^+ W^-$ and $e^+ e^- \rightarrow Z Z$* , *Z. Phys. C* **1** (1979) 259.
- [14] K. Hagiwara, R. D. Peccei, D. Zeppenfeld and K. Hikasa, *Probing the Weak Boson Sector in $e^+ e^- \rightarrow W^+ W^-$* , *Nucl. Phys. B* **282** (1987) 253.
- [15] M. Pospelov and T. ter Veldhuis, *Direct and indirect limits on the electromagnetic form-factors of WIMPs*, *Phys. Lett. B* **480** (2000) 181 [[hep-ph/0003010](#)].
- [16] K. Sigurdson, M. Doran, A. Kurylov, R. R. Caldwell and M. Kamionkowski, *Dark-matter electric and magnetic dipole moments*, *Phys. Rev. D* **70** (2004) 083501 [[astro-ph/0406355](#)].
- [17] E. Masso, S. Mohanty and S. Rao, *Dipolar Dark Matter*, *Phys. Rev. D* **80** (2009) 036009 [[0906.1979](#)].
- [18] S. Chang, N. Weiner and I. Yavin, *Magnetic Inelastic Dark Matter*, *Phys. Rev. D* **82** (2010) 125011 [[1007.4200](#)].
- [19] V. Barger, W.-Y. Keung and D. Marfatia, *Electromagnetic properties of dark matter: Dipole moments and charge form factor*, *Phys. Lett. B* **696** (2011) 74 [[1007.4345](#)].
- [20] T. Banks, J.-F. Fortin and S. Thomas, *Direct Detection of Dark Matter Electromagnetic Dipole Moments*, [1007.5515](#).
- [21] C. M. Ho and R. J. Scherrer, *Anapole Dark Matter*, *Phys. Lett. B* **722** (2013) 341 [[1211.0503](#)].
- [22] E. Del Nobile, C. Kouvaris, P. Panci, F. Sannino and J. Virkajarvi, *Light Magnetic Dark Matter in Direct Detection Searches*, *JCAP* **08** (2012) 010 [[1203.6652](#)].
- [23] J. Kopp, L. Michaels and J. Smirnov, *Loopy Constraints on Leptophilic Dark Matter and Internal Bremsstrahlung*, *JCAP* **04** (2014) 022 [[1401.6457](#)].
- [24] A. Ibarra and S. Wild, *Dirac dark matter with a charged mediator: a comprehensive one-loop analysis of the direct detection phenomenology*, *JCAP* **05** (2015) 047 [[1503.03382](#)].
- [25] T. Hambye and X.-J. Xu, *Dark matter electromagnetic dipoles: the WIMP expectation*, [2106.01403](#).
- [26] J. Hisano, A. Ibarra and R. Nagai, *Direct detection of vector dark matter through electromagnetic multipoles*, *JCAP* **10** (2020) 015 [[2007.03216](#)].
- [27] E. Del Nobile, G. B. Gelmini, P. Gondolo and J.-H. Huh, *Direct detection of Light Anapole and Magnetic Dipole DM*, *JCAP* **06** (2014) 002 [[1401.4508](#)].
- [28] M. Garny, A. Ibarra and S. Vogl, *Signatures of Majorana dark matter with t -channel mediators*, *Int. J. Mod. Phys. D* **24** (2015) 1530019 [[1503.01500](#)].
- [29] L. G. Cabral-Rosetti, M. Mondragón and E. Reyes-Pérez, *Anapole moment of the lightest neutralino in the cMSSM*, *Nucl. Phys. B* **907** (2016) 1 [[1504.01213](#)].
- [30] T. Abe, M. Fujiwara and J. Hisano, *Loop corrections to dark matter direct detection in a pseudoscalar mediator dark matter model*, *JHEP* **02** (2019) 028 [[1810.01039](#)].

- [31] P. Sandick, K. Sinha and F. Teng, *Simplified Dark Matter Models with Charged Mediators: Prospects for Direct Detection*, *JHEP* **10** (2016) 018 [[1608.00642](#)].
- [32] S. Kang, S. Scopel, G. Tomar, J.-H. Yoon and P. Gondolo, *Anapole Dark Matter after DAMA/LIBRA-phase2*, *JCAP* **11** (2018) 040 [[1808.04112](#)].
- [33] M. J. Baker and A. Thamm, *Leptonic WIMP Coannihilation and the Current Dark Matter Search Strategy*, *JHEP* **10** (2018) 187 [[1806.07896](#)].
- [34] C. Arina, A. Cheek, K. Mimasu and L. Pagani, *Light and Darkness: consistently coupling dark matter to photons via effective operators*, *Eur. Phys. J. C* **81** (2021) 223 [[2005.12789](#)].
- [35] J.-L. Kuo, M. Pospelov and J. Pradler, *Terrestrial probes of electromagnetically interacting dark radiation*, *Phys. Rev. D* **103** (2021) 115030 [[2102.08409](#)].
- [36] W. A. Bardeen, R. Gastmans and B. E. Lautrup, *Static quantities in Weinberg's model of weak and electromagnetic interactions*, *Nucl. Phys. B* **46** (1972) 319.
- [37] E. S. Abers and B. W. Lee, *Gauge Theories*, *Phys. Rept.* **9** (1973) 1.
- [38] K. Fujikawa, B. W. Lee and A. I. Sanda, *Generalized renormalizable gauge formulation of spontaneously broken gauge theories*, *Phys. Rev. D* **6** (1972) 2923.
- [39] S. Y. Lee, *Higher-order corrections to leptonic processes and the renormalization of weinberg's theory of weak interactions in the unitary gauge*, *Phys. Rev. D* **6** (1972) 1701.
- [40] M. J. Musolf and B. R. Holstein, *Observability of the anapole moment and neutrino charge radius*, *Phys. Rev. D* **43** (1991) 2956.
- [41] J. Papavassiliou and C. Parrinello, *Gauge invariant top quark form-factors from e^+e^- experiments*, *Phys. Rev. D* **50** (1994) 3059 [[hep-ph/9311284](#)].
- [42] L. G. Cabral-Rosetti, G. Lopez Castro and J. Pestieau, *One loop electroweak corrections to the muon anomalous magnetic moment using the pinch technique*, [hep-ph/0211437](#).
- [43] J. Bernabeu, G. A. Gonzalez-Sprinberg, J. Papavassiliou and J. Vidal, *Tau anomalous magnetic moment form-factor at super B/flavor factories*, *Nucl. Phys. B* **790** (2008) 160 [[0707.2496](#)].
- [44] J. M. Cornwall and J. Papavassiliou, *Gauge Invariant Three Gluon Vertex in QCD*, *Phys. Rev. D* **40** (1989) 3474.
- [45] J. Papavassiliou, *Gauge Invariant Proper Selfenergies and Vertices in Gauge Theories with Broken Symmetry*, *Phys. Rev. D* **41** (1990) 3179.
- [46] J. Bernabeu, L. G. Cabral-Rosetti, J. Papavassiliou and J. Vidal, *On the charge radius of the neutrino*, *Phys. Rev. D* **62** (2000) 113012 [[hep-ph/0008114](#)].
- [47] A. Rosado, *Physical electroweak anapole moment for the neutrino*, *Phys. Rev. D* **61** (1999) 013001.
- [48] J. Bernabeu, J. Papavassiliou and J. Vidal, *The Neutrino charge radius is a physical observable*, *Nucl. Phys. B* **680** (2004) 450 [[hep-ph/0210055](#)].
- [49] D. Binosi and J. Papavassiliou, *Pinch Technique: Theory and Applications*, *Phys. Rept.* **479** (2009) 1 [[0909.2536](#)].
- [50] A. Denner, G. Weiglein and S. Dittmaier, *Gauge invariance of Green functions: Background field method versus pinch technique*, *Phys. Lett. B* **333** (1994) 420 [[hep-ph/9406204](#)].

- [51] S. Hashimoto, J. Kodaira, Y. Yasui and K. Sasaki, *The Background field method: Alternative way of deriving the pinch technique's results*, *Phys. Rev. D* **50** (1994) 7066 [[hep-ph/9406271](#)].
- [52] J. Papavassiliou, *On the connection between the pinch technique and the background field method*, *Phys. Rev. D* **51** (1995) 856 [[hep-ph/9410385](#)].
- [53] A. Denner, G. Weiglein and S. Dittmaier, *Application of the background field method to the electroweak standard model*, *Nucl. Phys. B* **440** (1995) 95 [[hep-ph/9410338](#)].
- [54] A. Denner, H. Eck, O. Hahn and J. Kublbeck, *Feynman rules for fermion number violating interactions*, *Nucl. Phys. B* **387** (1992) 467.
- [55] A. Denner, H. Eck, O. Hahn and J. Kublbeck, *Compact Feynman rules for Majorana fermions*, *Phys. Lett. B* **291** (1992) 278.
- [56] R. Mertig, M. Böhm and A. Denner, *FeynCalc - computer-algebraic calculation of feynman amplitudes*, *Computer Physics Communications* **64** (1991) 345.
- [57] V. Shtabovenko, R. Mertig and F. Orellana, *New Developments in FeynCalc 9.0*, *Comput. Phys. Commun.* **207** (2016) 432 [[1601.01167](#)].
- [58] V. Shtabovenko, R. Mertig and F. Orellana, *FeynCalc 9.3: New features and improvements*, *Comput. Phys. Commun.* **256** (2020) 107478 [[2001.04407](#)].
- [59] V. Shtabovenko, *FeynHelpers: Connecting FeynCalc to FIRE and Package-X*, *Comput. Phys. Commun.* **218** (2017) 48 [[1611.06793](#)].
- [60] H. H. Patel, *Package-X: A Mathematica package for the analytic calculation of one-loop integrals*, *Comput. Phys. Commun.* **197** (2015) 276 [[1503.01469](#)].
- [61] K. Griest and D. Seckel, *Three exceptions in the calculation of relic abundances*, *Phys. Rev. D* **43** (1991) 3191.
- [62] M. J. Baker et al., *The Coannihilation Codex*, *JHEP* **12** (2015) 120 [[1510.03434](#)].
- [63] R. Flores, K. A. Olive and S. Rudaz, *Radiative Processes in Lsp Annihilation*, *Phys. Lett. B* **232** (1989) 377.
- [64] M. Garny, A. Ibarra and S. Vogl, *Dark matter annihilations into two light fermions and one gauge boson: General analysis and antiproton constraints*, *JCAP* **04** (2012) 033 [[1112.5155](#)].
- [65] S. P. Martin, *Compressed supersymmetry and natural neutralino dark matter from top squark-mediated annihilation to top quarks*, *Phys. Rev. D* **75** (2007) 115005 [[hep-ph/0703097](#)].
- [66] H. K. Dreiner, M. Kramer and J. Tattersall, *How low can SUSY go? Matching, monojets and compressed spectra*, *EPL* **99** (2012) 61001 [[1207.1613](#)].
- [67] ATLAS collaboration, *Search for direct stau production in events with two hadronic τ -leptons in $\sqrt{s} = 13$ TeV pp collisions with the ATLAS detector*, *Phys. Rev. D* **101** (2020) 032009 [[1911.06660](#)].
- [68] M. Berggren, *Stau searches at LEP*, *Nucl. Phys. B Proc. Suppl.* **98** (2001) 342.
- [69] B. C. Allanach and T. Cridge, *The Calculation of Sparticle and Higgs Decays in the Minimal and Next-to-Minimal Supersymmetric Standard Models: SOFTSUSY4.0*, *Comput. Phys. Commun.* **220** (2017) 417 [[1703.09717](#)].
- [70] G. Belanger, F. Boudjema, A. Pukhov and A. Semenov, *micrOMEGAs_3: A program for calculating dark matter observables*, *Comput. Phys. Commun.* **185** (2014) 960 [[1305.0237](#)].

- [71] G. Alguero, J. Heisig, C. Khosa, S. Kraml, S. Kulkarni, A. Lessa et al., *Constraining new physics with SModelS version 2*, [2112.00769](#).
- [72] P. Bechtle, O. Brein, S. Heinemeyer, O. Stal, T. Stefaniak, G. Weiglein et al., *HiggsBounds-4: Improved Tests of Extended Higgs Sectors against Exclusion Bounds from LEP, the Tevatron and the LHC*, *Eur. Phys. J. C* **74** (2014) 2693 [[1311.0055](#)].
- [73] O. Stal and T. Stefaniak, *Constraining extended Higgs sectors with HiggsSignals*, *PoS EPS-HEP2013* (2013) 314 [[1310.4039](#)].
- [74] F. Mahmoudi, *SuperIso v3.0, flavor physics observables calculations: Extension to NMSSM*, *Comput. Phys. Commun.* **180** (2009) 1718.
- [75] P. Athron, M. Bach, H. G. Fargnoli, C. Gnendiger, R. Greifenhagen, J.-h. Park et al., *GM2Calc: Precise MSSM prediction for $(g - 2)$ of the muon*, *Eur. Phys. J. C* **76** (2016) 62 [[1510.08071](#)].
- [76] A. Buckley, *PySLHA: a Pythonic interface to SUSY Les Houches Accord data*, *Eur. Phys. J. C* **75** (2015) 467 [[1305.4194](#)].
- [77] B. C. Allanach et al., *SUSY Les Houches Accord 2*, *Comput. Phys. Commun.* **180** (2009) 8 [[0801.0045](#)].
- [78] R. H. Helm, *Inelastic and Elastic Scattering of 187-Mev Electrons from Selected Even-Even Nuclei*, *Phys. Rev.* **104** (1956) 1466.
- [79] J. Lewin and P. Smith, *Review of mathematics, numerical factors, and corrections for dark matter experiments based on elastic nuclear recoil*, *Astropart. Phys.* **6** (1996) 87.
- [80] XENON collaboration, *Dark Matter Search Results from a One Ton-Year Exposure of XENON1T*, *Phys. Rev. Lett.* **121** (2018) 111302 [[1805.12562](#)].
- [81] SUPERCDMS collaboration, *Search for Low-Mass Weakly Interacting Massive Particles with SuperCDMS*, *Phys. Rev. Lett.* **112** (2014) 241302 [[1402.7137](#)].
- [82] PICO collaboration, *Dark Matter Search Results from the Complete Exposure of the PICO-60 C₃F₈ Bubble Chamber*, *Phys. Rev. D* **100** (2019) 022001 [[1902.04031](#)].
- [83] XENON collaboration, *Physics reach of the XENON1T dark matter experiment*, *JCAP* **04** (2016) 027 [[1512.07501](#)].
- [84] J. P. Ellis, *Tikz-feynman: Feynman diagrams with tikz*, *Computer Physics Communications* **210** (2017) 103.
- [85] H. E. Haber and G. L. Kane, *The Search for Supersymmetry: Probing Physics Beyond the Standard Model*, *Phys. Rept.* **117** (1985) 75.
- [86] M. Drees, R. Godbole and P. Roy, *Theory and Phenomenology of Sparticles: An Account of Four-Dimensional $N = 1$ Supersymmetry in High Energy Physics*. World Scientific, 01, 2005, [10.1142/4001](#).